P1.11

THE CERES GEOSTATIONARY CALIBRATION METHODOLOGY WITH EMPHASIS ON THE DESERT CALIBRATION

Rajendra Bhatt*, D. L. Morstad, and A. Gopalan
Science Systems and Applications, Inc., Hampton, VA 23666

D. R. Doelling
NASA Langley Research Center, Hampton, VA 23666

1 INTRODUCTION

The Clouds and the Earth's Radiant Energy System (CERES) project provides the community with quality climate TOA and surface fluxes and cloud properties which are key elements in evaluating the ability of climate models to predict both past and future climate states. One important aspect of successful climate monitoring is post-launch calibration and characterization of satellite instruments. The CERES instantaneous broadband calibration radiance stability is 0.2% per year, whereas the accuracy of the longwave (LW) and shortwave (SW) is better than 0.5% and 1% respectively (Priestley et al, 2006). The CERES TOA broadband flux record also incorporates 3-hourly geostationary (GEO) fluxes and cloud products to derive broadband fluxes and cloud properties that fill the gap between CERES measurements onboard the sun-synchronous Terra (10:30 AM) and Aqua (1:30 PM) orbits. In order to combine the CERES and GEO radiances in one product, they must both be on a consistent radiometric scale.

The GEO visible channels do not have onboard calibration. Therefore, in order to be incorporated with CERES products for monitoring climate, these channels must be vicariously calibrated. In order to have consistent calibration across all 5 geostationary satellites surrounding the earth, MODIS is used as a calibration reference. This will allow seamless GEO retrieved cloud properties across satellite boundaries. These GEO cloud retrievals are then used to derive the scene identification to convert the NB GEO radiance into BB radiance and into BB fluxes using the CERES ADM. A ray-matching technique then inter-calibrates the GEO radiances with MODIS. The GEO sensor degradation based on inter-calibration with MODIS is then validated against desert calibration. The two methods should be consistent. The CERES team also uses deep convective clouds as an invariant target to monitor the degradation of the GEO visible sensor. This paper focuses on the NASA-Langley GEO desert calibration technique.

**Corresponding author address*: Rajendra Bhatt, SSAI, 1 Enterprise Pkwy, Hampton, VA 23666.
email: Rajendra.Bhatt@nasa.gov

2 RAY-MATCHING TECHNIQUE

The ray-matching technique uses MODIS as an absolute calibration reference and then using coincident bore sighted radiances to transfer the calibration. Following the approach of Minnis et al 2008, this technique uses coincident, co-angled, and co-located pixel radiances to transfer the calibration from a well-calibrated satellite sensor to another. The GEO raw counts (proportional to radiance) and MODIS radiances are binned within 0.5° x 0.5° over ±20°E, W and ±15° N, S ocean region near the sub-satellite point. Any land pixels over the calibration domain are masked, because the spectral signature over land is unpredictable. As ocean and clouds are mostly spectrally flat, no spectral corrections are made to account for the difference in relative spectral responses of MODIS and GEO channels. The solar, viewing, and azimuth angles of the two satellites are matched within 5° (15 minutes), 10°, and 15° respectively. Ray-matched gridded GEO raw counts are regressed against MODIS radiances and gains are derived on a monthly basis (Figure 1). Since the GEO satellites maintain space as a constant offset, the published space count is used in the regression equation. For Meteosat-9 it is 51 digital counts out of a 10-bit count resolution. Figure 1 indicates that the regression gave an offset of 51.5 (XoffPC) confirming the fact that the Meteosat-9 and MODIS spectral response functions observe similar reflectances over cloudy ocean scenes. The gain is 0.5461 for April 2010, for a solar constant of 526.9 $Wm^{-2}\mu m^{-1}sr^{-1}$. The published Meteosat-8 solar constant is 515.0 $Wm^{-2}\mu m^{-1}sr^{-1}$ (Govearts and Clerici 2004), should be very similar to Meteosat-9. The most recent EUMETSAT 0.64µm channel Meteosat-9 calibration is 0.514 for December 2009, available at the following web page (http://www.eumetsat.int/Home/Main/Access_to_Data/Meteosat_Meteorological_Products/Calibration/SP_1119512219822?l=en, and located in the document pdf_ten_052058_msg1_vis6_calib.pdf). After adjusting for the solar constant difference the ray-matching technique based on Terra-MODIS is 4% greater than EUMETSAT. The Meteosat-9 0.65µm radiance is computed as Rad = gain*(Count – space count).

In order to trend the GEO instrument response over time, the computed monthly gains are plotted as a function of time (Figure 2). The time is measured in days since launch (DSL). Meteosat-9 became operational in April 2007. To compute the gain for a particular day use, gain = OFF + DSL*SLOPE. For Meteosat-9 the degradation is ~0.15% per year and appears to be linear.

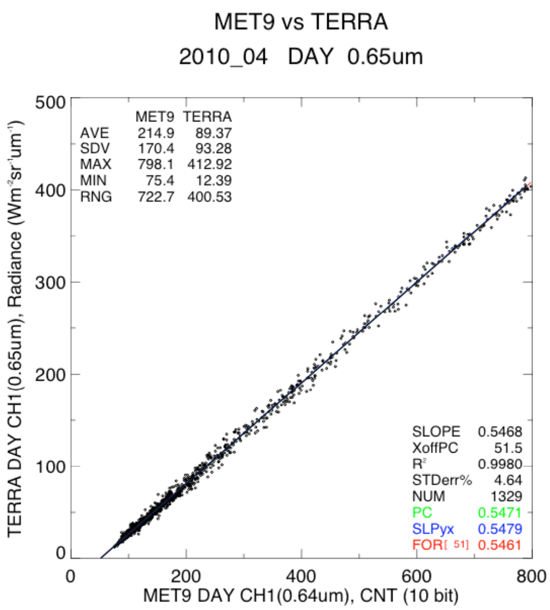

Fig. 1. Monthly scatter plot of MODIS radiance vs ray-matched gridded Meteosat-9 raw counts.

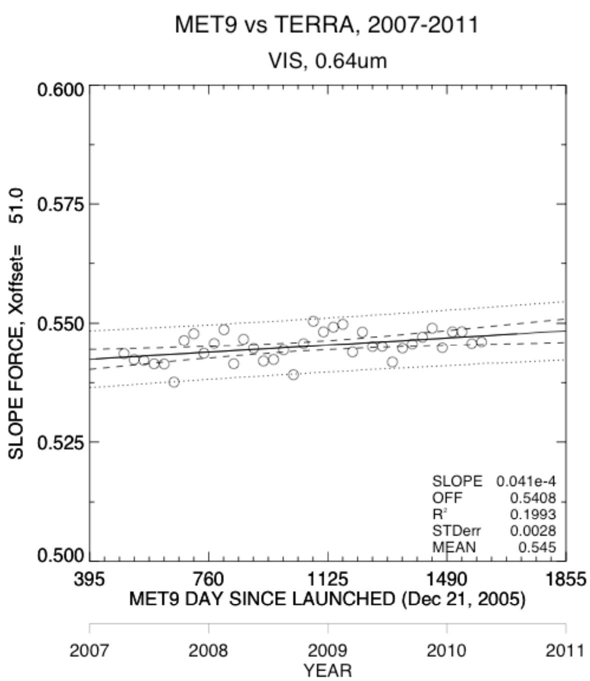

Fig. 2. Meteosat-9 visible trend derived from ray-matched intercalibration technique.

3 INVARIANT DESERT SITE TECHNIQUE

Invariant desert sites on Earth have been used often to characterize the in-orbit radiometric stability of satellite instruments. The underlying assumption for this technique is that the reflectance of these ground targets remains constant over time, and any change observed in satellite instrument response to these targets over time would be due to the degradation of the instrument itself. This paper uses Saharan and Arabian deserts and demonstrates the proof of concept as applied to the Meteosat-9 visible channel.

The Saharan and Arabian deserts are large and spatially homogeneous (Teillet et. al. 2007). This is required to minimize the error due to scene-to-scene misregistration. Additionally, these targets are very bright and arid, resulting in reduced atmospheric impact on upwelling radiation. The three desert sites selected for this study are Libya 4 (1.5° x 1.5° region-of-interest centered around 28.75° lat and 23.25°E lon), Arabia 2 (1.5° x 1.5° region-of-interest centered around 20.25° lat and 51.00°E lon), and Egypt 1 (0.6° x 0.6° region-of-interest centered around 27.00° lat and 26.30°E lon). Figure 3 shows the three desert sites as viewed by the Meteosat-9 visible channel.

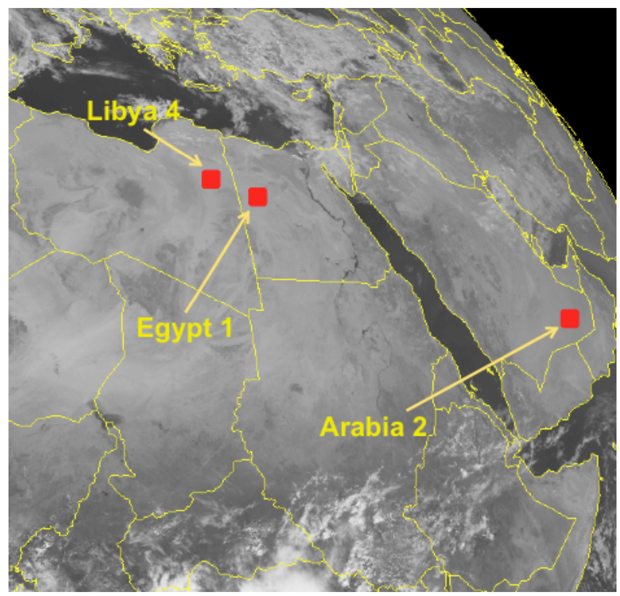

Fig. 3. Meteosat-9 visible image showing Saharan and Arabian desert sites.

The Meteosat-9 visible pixel raw counts acquired over each region of interest were averaged after subtracting the space count (zero radiance). Local noontime is chosen for Meteosat-9 data, as the upwelling radiation is very high because of shorter path length for solar irradiance. This provides higher signal-to-noise ratio (SNR), and reduces uncertainties due to atmospheric effects. Although these deserts remain cloud free most of the time, a filter based on spatial standard deviation was used to eliminate any cloudy scenes. On a clear-sky day, the spatial standard deviation of these homogeneous regions is rather low, and any increase to the standard deviation can be attributed to the presence of a cloud. The threshold was determined by visible inspection after looking at the spatial standard deviation profile on clear-sky days (Figure 4).

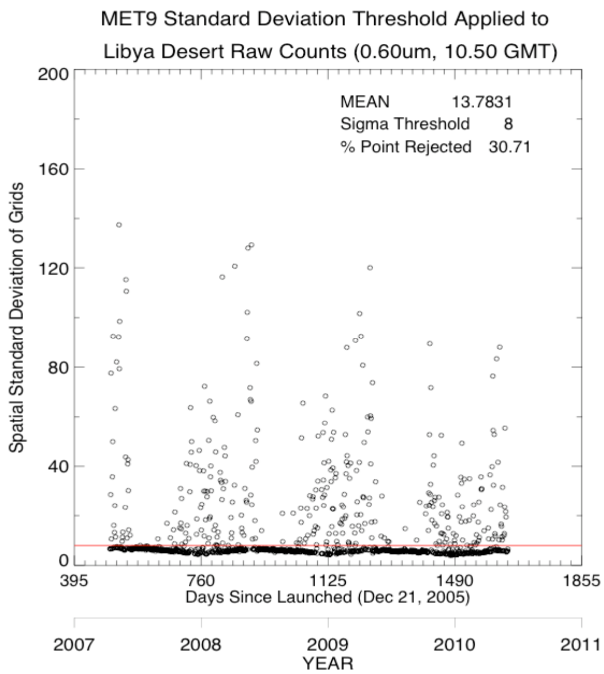

Fig. 4. Daily clear-sky identification based on spatial standard deviation.

After eliminating cloudy scenes, the daily mean raw counts are averaged on a monthly basis for consistency with GEO-to-MODIS intercalibration. Figure 5 shows the monthly means plotted against days since launch (DSL). The seasonal cycles displayed in Figure 5 can be attributed to the variation of solar geometry throughout a year. In order to reveal the true instrument response, the monthly mean raw counts must be appropriately de-seasonalized. To do this, first a 12-month running mean is computed, second a relative ratio between the month and the running mean is determined, third a average relative ratio for each of the 12 months is computed, this climatology ratio is then applied to de-seasonalize all the monthly raw counts for the time period. This methodology needs at least 2 years of data, however it can determine both linear and nonlinear trends degradation rates of various magnitudes consistent with the ray-matched technique.

The de-seasonalized means are then plotted against DSL to get the relative stability of Meteosat-9 visible channel over its lifetime (Figure 6). The standard error of estimate is less than 0.6% of the mean, which shows that the de-seasonalization technique has worked well. Note that the downward trend in Figure 6 is consistent with the upward trend of the gain in the GEO/MODIS inter-calibration in Figure 2, since it is a correction to the degradation of the satellite instrument assuming the desert is stable. The next step from here is to compare the consistency between this trend line and the one obtained from GEO-to-MODIS ray-matched technique. This can be done through normalization of the two trend lines and anchoring them at the mid DSL point.

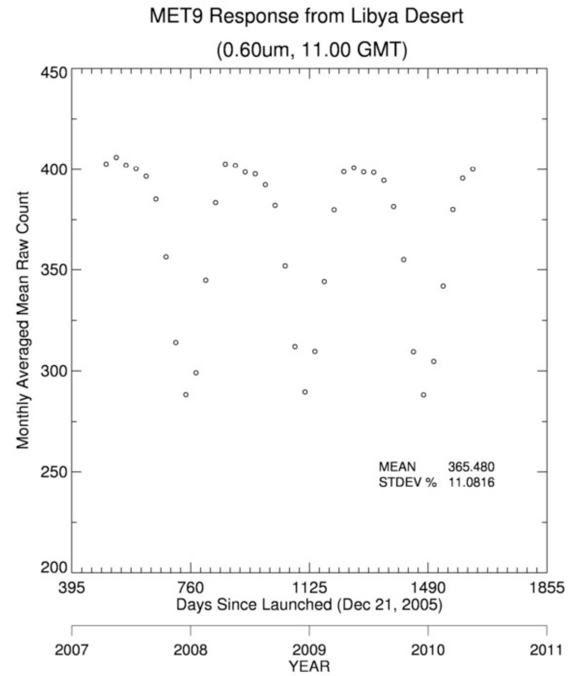

Fig. 5. Seasonal variation of monthly mean raw counts of Meteosat-9 over Libya 4 desert.

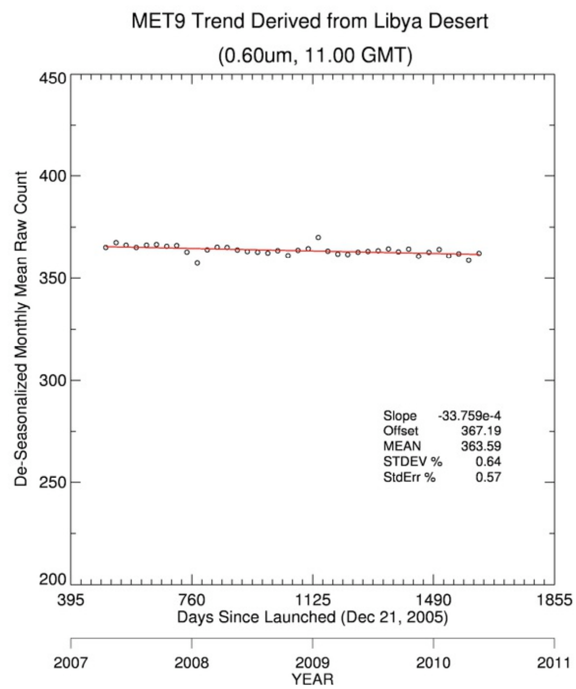

Fig. 6. De-seasonalized monthly mean raw counts reveal long-term stability of Meteosat-9 visible channel.

4 RESULTS

Disadvantages of using deserts sites include variance of the atmospheric column transmission due to water vapor, aerosols and thin clouds. This method assumes that the clearest or greatest transmission cases are those with the lowest spatial standard deviation. Adding aerosols and clouds would increase the spatial standard deviation. This is evident since there is bottom shelf (Figure 4) on the standard deviation, which is the usual pristine condition. This method relies on the average pristine condition to maximize the number of days over the time period. For the Libyan desert 70% of all days were used, whereas the Egyptian and Arabian sites was 80%. Humidity, a function of near surface air temperature, is essentially a seasonal variation over deserts, taken out by deseasonalization. Monitoring deserts with visible sensors onboard GEO satellites imposes a periodic variation of solar zenith angle (SZA) both seasonally and diurnally, although the view zenith angle (VZA) is constant. The GEO satellites follow a strict operational schedule, there by ensuring an annual repeatable solar geometry cycle. Each desert has a unique surface spectral and bidirectional reflectance (BDRF) signal. The annual SZA cycle with its accompanying BDRF effects on the radiance are easily taken out using deseasonalization.

If this desert calibration method is robust it should give the same relative degradation no matter which local time is used. The Libyan desert site also contains sand dunes with a specific orientation, causing diurnally varying shadows at the given VZA. From the satellite perspective a desert site would change from forward and to backscatter as the local time crosses noon during the day. To test the impact of these issues, a comparison between three trend lines derived from Meteosat-9 noontime, morning (~ 9 AM local time), and afternoon (~ 3 PM local time) data over Libya 4 desert is shown in Figure 7. The relative degradation is computed by dividing the monthly deserts counts with the count on April 2007. They agree within 0.3% over 3 years validating the desert calibration methodology. Desert calibration using the local noon image provides the smallest standard error of 0.57% because of minimum atmospheric impact (shortest path length) and high signal-to-noise ratio (minimum SZA). This is evident by the increased number of monthly outliers of the morning and afternoon image times in Figure 7.

Another disadvantage of using deserts is the claim that they are invariant over time, especially over long time scales. Desert sites for this study were chosen to contain no vegetation, surface water, or snow. However if one monitors several desert sites in differing synoptic regions over the same GEO domain, a desert site that is changing reflectance over a short period of time can be identified.

Figure 8 shows the comparison of Meteosat-9 visible channel response trends derived from GEO-to-MODIS ray-matched and invariant desert site techniques applied to Libya 4, Arabia 2 and Egypt 1 desert sites respectively. The black solid line is MODIS-based trend and the remaining lines are based on individual desert-based trends. The regression analysis done with the MODIS-based calibration shows an evidence of trend in Meteosat-9 visible band (p=0.0055). It indicates a degradation of about 0.8% over 3 years. The three desert trend lines are also consistent to GEO-to-MODIS trend line within 0.5% over the same period. Similarly, the three desert sites agree within 0.6%. Egypt 1 displays the lowest noise of the three desert sites with a standard error of estimate of about 0.52%. Consistency

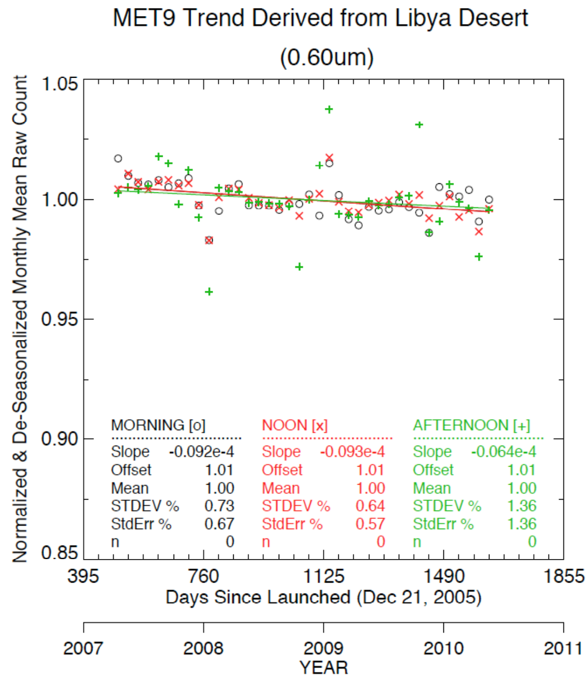

Fig. 7. Comparison of three trend lines obtained from Meteosat-9 using local noon, morning and afternoon data.

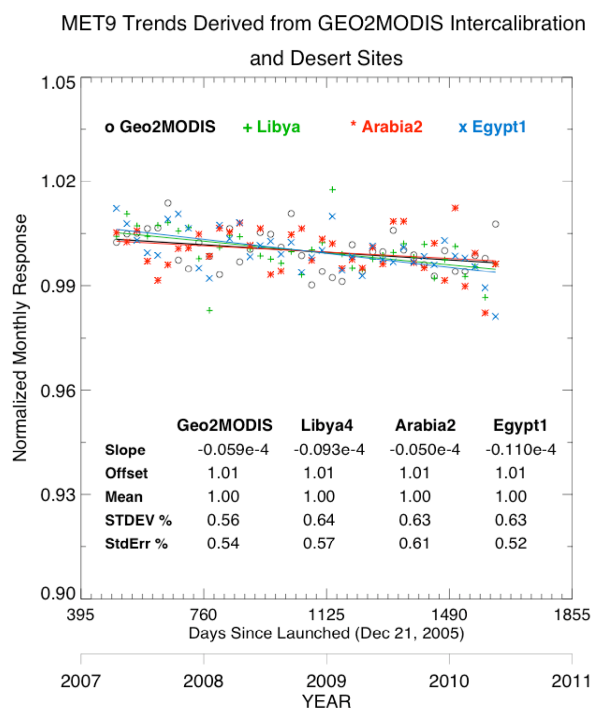

Fig. 8. Comparison between GEO-to-MODIS ray-matched and invariant desert site technique for Meteosat-9 visible channel; (a) Libya 4, (b) Arabia 2, (c) Egypt 1 desert sites.

among desert targets indicates they are invariant and the desert calibration method is robust.

Another way to monitor the stability of a given desert and the robustness of this desert calibration technique is to use the same desert viewed by two GEO satellites. If the GEO/MODIS calibration is applied to the given desert site counts for each GEO satellite and the resulting radiance is then normalized at the middle of the time record, the stability of the desert should be consistent among GEO platforms. Figure 9 shows the Libyan desert normalized radiance for both Meteosat-7 and 9. Note how remarkable the monthly desert radiances from both GEO satellites track each other, especially the outliers. Also the resultant trends are within 0.1%, demonstrating the robustness of the desert calibration technique in removing annual SZA variations. If the GEO/MODIS calibration is consistent, then any periodic or long term trending is due to the desert itself.

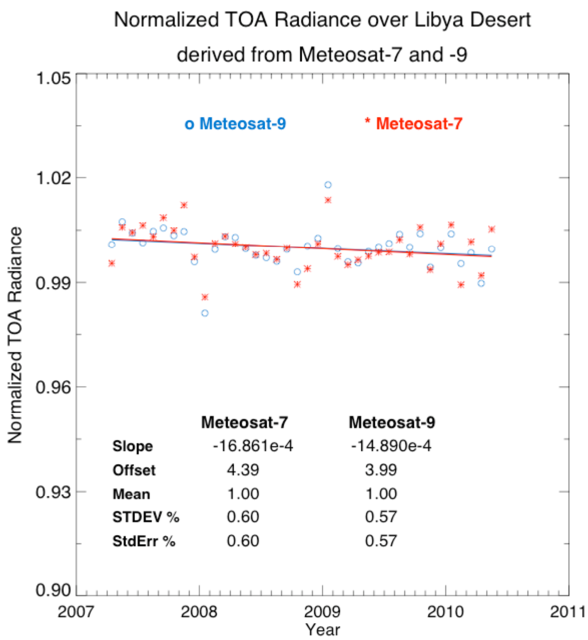

Fig. 9. Comparison of the Libyan desert radiances from Meteosat 7 and 9 and using inter-calibration gains based on Terra-MODIS. Slope is given in years^{-1}.

5 CONCLUDING REMARKS

A methodology has been developed based on invariant desert sites that can be used to validate the existing ray-matched GEO-to-MODIS inter-calibration technique. The target stability is of critical importance for this technique, and can be monitored by incorporating multiple (independent) deserts site over the same GEO domain and using two GEO satellites to track the same desert. Incorporating the noontime images and deseaonalization can easily reduce the atmospheric and BDRF impacts. This methodology will be further incorporated for other geostationary satellites. The derived trend lines will also be validated in the future using deep-convective cloud techniques.

6 ACKNOWLEDGEMENTS

The NASA science mission directory through the CERES project at the NASA-Langley research center funded this research.

7 REFERENCES

Govearts, Y. and M. Clerici, 2004: MSG-1/SEVIRI Solar Channels Calibration Commissioning Activity Report, EUM/MS/TEN/04/0024, available at EUMETSAT web site (see text).

Minnis, P., D. R. Doelling, L. Nguyen, W. F. Miller, V. Chakrapani, 2008, Assessment of the Visible Channel Calibrations of the VIRS on TRMM and MODIS on Terra and Aqua, J. Atmos. Oceanic Technol., 25, 385-400

Priestley, K. J., G. Matthews, S. Thomas, D. Cooper, D. Walikainen, P. Hess, Z. P. Szewczyk, and R. Wilson, 2006: Proc. AMS 12th Conference on Atmospheric Radiation, Madison, WI, July 10-14

Teillet, P.M., Barsi, J.A., Chander, G., Thome, K.J., 2007: Prime Candidate Earth Targets for the Post-Launch Radiometric Calibration of Space-Based Optical Imaging Instruments, *Proc. Of SPIE Vol. 6677, 66770S, (2007).*